

Thermal simulation and experimental results of a micromachined thermal inclinometer

J. Courteaud^{a,*}, P. Combette^a, N. Crespy^a, G. Cathebras^b, A. Giani^a

^a Institut d'électronique du Sud, UMR 5214 Université Montpellier II/CNRS,
Place E. Bataillon, 34095 Montpellier Cedex 5, France

^b Laboratoire d'informatique de Robotique et de Micro-électronique de Montpellier,
UMR 5506 Université Montpellier II/CNRS, 161 rue Ada, 34392 Montpellier Cedex 5, France

Received 2 July 2007; accepted 5 September 2007

Available online 18 September 2007

Abstract

This paper presents a numerical simulation and experimental results of a one-dimensional thermal inclinometer with sensitivity studies and optimization. The sensor principle consists of one heating resistor placed between two detectors. When the resistor is electrically powered, it creates a symmetrical temperature profile inside a micromachined silicon cavity. By applying a tilt to the sensor, the profile shifts in the same direction of the sensible axis corresponding to the horizontal one-to-one. The temperature profile and the sensitivity according to the CO₂ gas pressure have been studied using numerical resolution of fluid dynamics equations with the computational fluid dynamics (CFD) software package Fluent V6.2. The influence of the temperature on the thermo-physical fluid properties has been examined. We have shown that the isothermal temperature profile decreases while the pressure increase. A maximum of the sensitivity at 11 bar for CO₂ gas pressure has been obtained taken into consideration of the sensor geometry. Two models have been used to evaluate the thermal boundary layer size function of the evolution of the pressure and theoretically extended to other gases in order to become a parameter field between gas and design. By using micromachined silicon technique, a thermal inclinometer with one pair of detectors placed at 300 μm from the heater has been made. Experimental measurements with CO₂ gas corroborate with the numerical simulation and for the optimum pressure, the sensitivity is respectively of 7 °C and 8.1 °C per angle of inclination (°) for an operating power of 75 mW corresponding to a 250 K rise of the heater temperature.

© 2007 Elsevier B.V. All rights reserved.

Keywords: Thermal inclinometer; Simulation; Micromachined silicon; Tilt measurements

1. Introduction

Inclinometer is a very sensitive accelerometer used in a low g application for tilt measurements. They are widely used in the field of aviation, automation (machine control and industrial process monitoring), seismic monitoring and more especially in automotive applications such as chassis regulation or active car suspension.

Most of the micromachined inclinometers currently used in electrical categories are capacitive or piezoresistive [1,2]. Their major disadvantage is the existence of the proof mass, which

induces a low shock survival rating. Main advantages of the thermal inclinometer studied are its small size (micromachined) inducing a low fabrication cost and a high shock reliability due to the absence of seismic mass. The principle of inertial sensors was first studied by Dao et al. [3–5]. The particular case of the inclinometer was studied by Billat et al. [6]. Fig. 1 shows the principle of the sensor, composed of one heating resistor placed between two detectors. Based on free convection in a close chamber containing a gas, the heating resistor creates a symmetrical temperature profile and a thermal balance inside the cavity. When an inclination is applied, the temperature profile shift and the balance are modified, creating a difference of temperature on the detectors $2\Delta T_{\text{detector}}$. To improve the sensitivity, the overall system is suspended (in the air) and the detectors are placed at 300 μm from the heater [7]. In this article, the thermal inclinometer response has been experimentally measured and quantitatively evaluated by using numerical resolution of fluid

* Corresponding author at: Centre d'électronique et de micro-optoélectronique de Montpellier (CEM2), UMR CNRS 5507, Université Montpellier II, Place Eugène Bataillon, Case Courrier 075, 34095 Montpellier, France.

Tel.: +33 4 67 14 37 84; fax: +33 4 67 54 71 34.

E-mail address: courteaud@cem2.univ-montp2.fr (J. Courteaud).

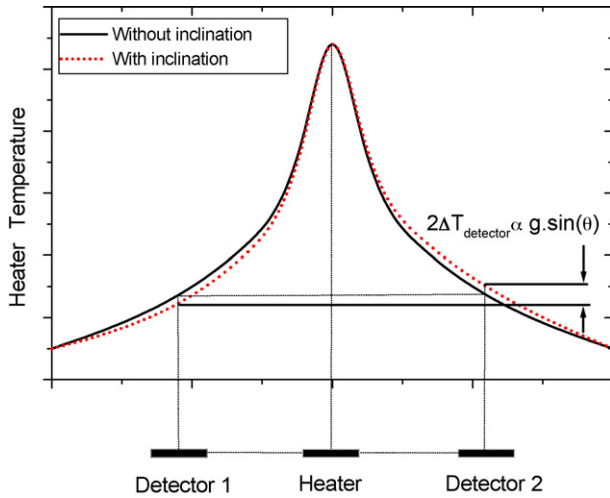


Fig. 1. Temperature profile with and without inclination.

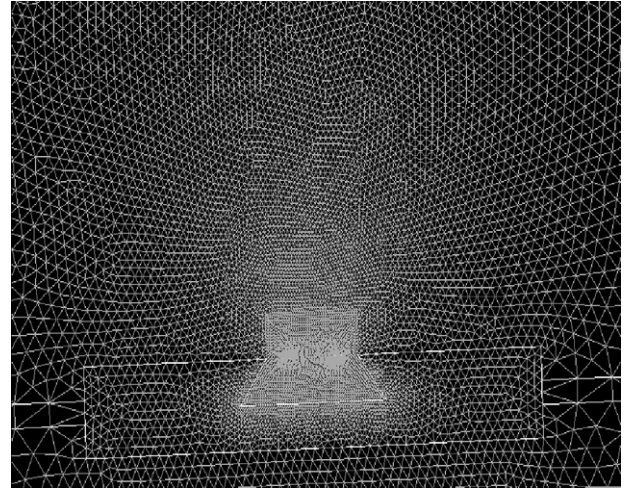


Fig. 3. Inclinator's meshing.

dynamic equations with the commercial code CFD Fluent V6.2 as a function of the gas pressure inside the cavity in order to improve the sensor sensitivity.

2. Microstructure design

2.1. Experimental design

Fig. 2 shows a scanning electron microscope (SEM) image of the device after the fabrication of the sensor. The silicon cavity size is $1000\ \mu\text{m} \times 2000\ \mu\text{m}$ and its depth is $400\ \mu\text{m}$. Details of the fabrication steps have been already described [7]. A thin platinum film has been used because of its good temperature coefficient (TCR) and its good physical properties, which enable more stability in time for high temperature. Heater and detectors widths are $100\ \mu\text{m}$ and $22\ \mu\text{m}$, respectively. Thin platinum film resistors deposited on low stress ($\sigma \approx 0$) Si-rich silicon nitride membrane SiN_x [8] have been used to improve the thermal resistance between the detector and the surrounding substrate and to limit the energy consumption. So the main results are

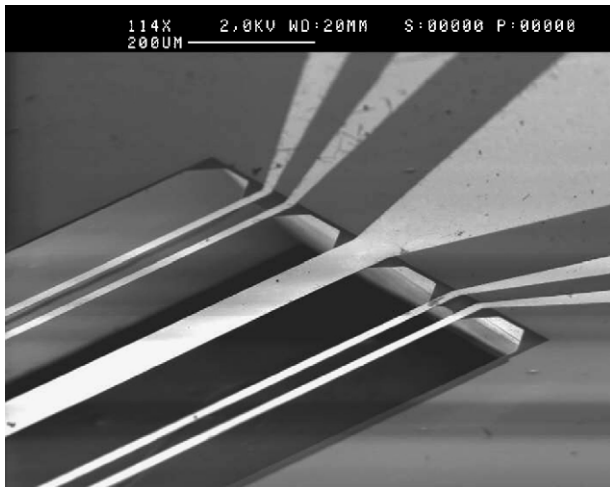


Fig. 2. SEM image of the sensor with heater and detectors.

hereafter reminded: Thickness of the SiN_x and platinum layers are 5000 and $3000\ \text{\AA}$ with Cr adhesion-promoting layer. Platinum was evaporated at 400°C with an electron beam and vacuum-annealed at 500°C . The electrical resistivity is about $15\ \mu\Omega\text{ cm}$ with a resistance temperature coefficient of (TCR) of $3.1 \times 10^{-3}/^\circ\text{C}$. The platinum resistors and the SiN_x are successively pattern by electron cyclotron resonance (ECR) etching. To obtain resistors on SiN_x bridges, the silicon is anisotropically etching out using KOH solution at 85°C . Finally, the tilt sensor is packaged in a cylindrical copper case in order to easily control the gas pressure, to induce a high thermal capacitance, and prevent external flow temperature perturbation.

2.2. Simulation design

The size of the silicon cell is the same as the experimental one. The whole space around the sensor is delimited by a cavity wall ($10\text{ mm} \times 10\text{ mm}$) at isothermal wall condition (ambient temperature at 300 K). The geometry used for these simulations is the same as the experimental shape taking into consideration Pt/ SiN_x total bilayers thickness of $1\ \mu\text{m}$. The triangular mesh structure is illustrated on Fig. 3. The meshing of the array has been adjusted near the heater and the detectors, in order to improve the density of calculation near the critical regions.

3. Theory of the inclinometer

3.1. Analytical theory

By using a simple model based on Grashof number (Gr) studied by Leung et al. [4], they suggest that the sensitivity of the thermal accelerometer is linearly proportional to this number. Since inclinometer is a particular case of a thermal accelerometer, so the sensitivity is proportional to:

$$Gr = \frac{\rho^2 g \beta (T_p - T_0) l^3}{\mu^2} \quad (1)$$

where g acceleration or gravity earth, ρ gas density, β gas coefficient of expansion, $\Delta T = (T_p - T_0)$, temperature difference between the heater and the environment (K), l , characteristic size and μ , gas viscosity.

As the accelerometer's sensitive axis is tilted from pointing horizontal to vertical, the influence of the gravity varies as a function of the sinus of the angle between the horizon and the accelerometer's sensitive axis thus inclinometer application. The relation between $2\Delta T_{\text{detector}}$ and the tilt angle θ is given by:

$$2\Delta T_{\text{detector}} \propto g \sin(\theta) \quad (2)$$

Since the sensors are convection-based, by working under higher gas pressure according to Gr number we achieve a higher sensitivity. The thermal inclinometer response has been studied using numerical resolution with a CFD Fluent code, in order to evaluate the temperature difference between the two detectors.

3.2. Thermal simulation of the inclinometer

3.2.1. Basic equation and computational techniques used

In this section, we remind the main basic equations, boundary and initial conditions which govern the problem. Navier–Stoke equations are solved and derived from conservation laws using the transformation described above and need to be close relation with state laws given by:

$$\nabla(\rho k) = \nabla(\Gamma_k \nabla k) + S_k \quad (3)$$

This equation describes the steady state of a quantity k , balanced by the ρ density, followed by the three components of spatial derivative. ∇f is the gradient of the scalar function f .

The continuity, momentum and energy equations are introduced in vectors form by:

$$\nabla v = 0 \quad (4)$$

$$\rho v \nabla v = -\nabla p + \rho g \beta (T_p - T_0) + \mu \nabla^2 v \quad (5)$$

$$\rho C_p v \nabla T = \lambda \nabla^2 T \quad (6)$$

These equations assume steady state flow of an incompressible fluid with negligible viscous dissipation where: v , the velocity, p , the fluid pressure, T , the temperature, μ , the viscosity, C_p , specific heat, λ , conductivity.

The sensor model is created in 2D. Computational grids were made by Gambit 2.0 (Fluent Inc.). The meshing of the array is adjusted to improve the density of calculation near the critical regions. Fluent 6.0 was used to simulate mass, momentum, and heat transfer by solving a set of non-linear governing equations in each cell. Computational fluid dynamic calculations are the Navier–Stokes equations, the continuity, the energy, and the momentum equations. The continuity equation essentially explains that the mass flow rate into a specific volume must be equal to the mass flow rate out of that volume (such volume can be one cell in the flow domain). This equation is used to ensure that CFD codes do not create extra fluid where it cannot and must not exist. The energy equation is used to determine that energy is neither created nor destroyed in the fluid system,

according to the third law of thermodynamics. The fluid model used is an ideal gas model with variable μ , λ , C_p . The initial guesses for velocity, temperature, and viscosity fields were set to constant values over the entire computational domain. The solver undertakes iteration until the convergence criterion is satisfied, using scaled residuals of the modified variables in the governing equations as the measure. In addition, isothermal wall heat flux was examined explicitly for convergence (to less than a 0.01% variation between iterations). The whole calculation domain is submitted to a gravity body force corresponding to the desired inclination angle.

4. Simulation and experimental results

4.1. Optimization of the sensitivity with gas under pressure

The sensor is placed in a hermetic chamber, and a manometer controls the gas pressure. The gas is nitrogen or helium with pressure ranges from 1 to 30 bar or CO₂ with a particular attention of this last one because of his low diffusivity characteristic, which increases the sensitivity. The temperature profile with zero degree of inclination on the sensitive axis is studied according to the different gas pressure with a focus on the CO₂ one for a constant heater temperature rise $\Delta T = 250$ K. The electrical value of the heater resistance is deducted from $R(T_{\circ C}) = U/I$ and its average temperature is calculated using the Eq. (7):

$$T_{\circ C} = \frac{R(T_{\circ C}) - R_{0\circ C}}{\alpha R_{0\circ C}} \quad (7)$$

Fig. 4 shows the necessary power supply to obtain a constant heater temperature rise ΔT according to the gas pressure. The measuring range goes from 60 mW at atmospheric pressure up to 75 mW for a CO₂ pressure of 15 bar and goes from 68 mW at atmospheric pressure up to 98 mW for N₂ pressure of 30 bar, respectively. For helium gas, the range from 190 to 210 mW at 30 bar pressure has been measured. In the low pressures range, the power consumption is fairly independent of the pressure but it increases for higher pressures because of the increase

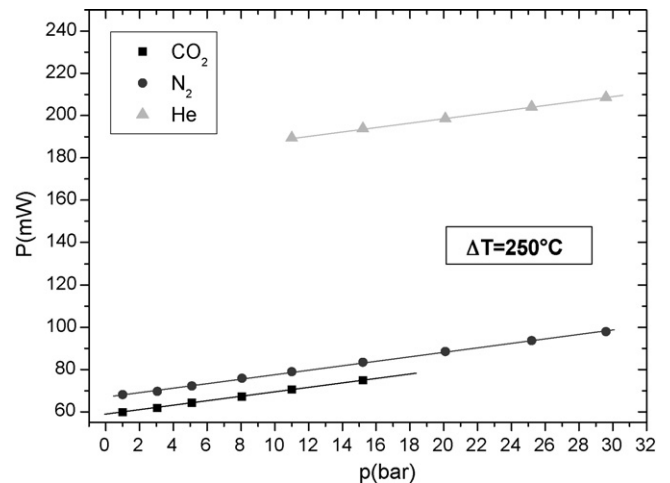


Fig. 4. Necessary supplied power to obtain a constant heater rise ($\Delta T = 250$ K) vs. gas pressure.

Table 1
Comparison of gases diffusivity at $\Delta T_{\max} = 563\text{ K}$

Gas	Air	Nitrogen	Carbon dioxide	Helium	Oxygen	Krypton	Xenon
$2\Delta T_{\text{detector}}/2\Delta T_{\text{detector}}(\text{air})$	1	1.014	3.04	0.014	0.872	4.3	11.5
Thermal diffusivity, $\alpha (\times 10^{-5}) (\text{m}^2/\text{s})$	6.786	6.738	3.892	56	7.264	3.542	2.184

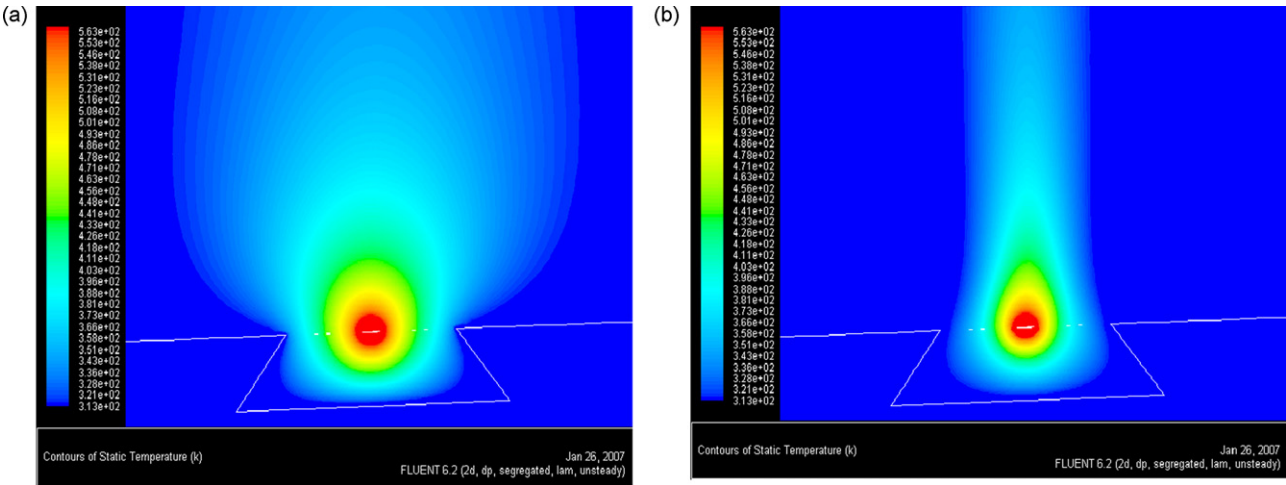


Fig. 5. Temperature profile for CO_2 gas at atmospheric (a) and 11 bar (b) pressure.

of heat losses. Table 1 summarized the comparison of thermal diffusivity for different gas at a $\Delta T_{\max} = 563\text{ K}$.

Let us focus on the CO_2 gas pressure to maximize the sensitivity. On Fig. 5a and b, the heat transfer or the temperature distribution shows a clearly reduction of the isothermal temperature profile. For 1 and 11 bar, the $2\Delta T_{\text{detector}}$ is equal to 0.102 and 8.1°C , respectively. In Fig. 6, we represent the experimental response of the sensor functions of CO_2 gas pressure. So, the $2\Delta T_{\text{detector}}$ has been numerically calculated only for this gas and experimentally measured for a variation of 1° of inclination according to nitrogen and helium gas pressure too. The results are plotted on log–log scale in Fig. 7. A linear variation proportional to the square of the pressure as predicted by Eq. (1) is

observed. For CO_2 gas, at around 9 bar, the sensitivity starts to saturate and decreases down to 15 bar. However, we can observe a lower difference between the simulation results and the experimental one. It certainly comes from the 2D modelling which introduce a lower divergence but the behaviour is similar.

Experimentally, the same phenomenon for high nitrogen gas pressure is also observed. It is probably due to the temperature profile, which narrows and moves out the detectors, so the thermal boundary layer δ_{th} decreases when the pressure is too important. This decrease of the thermal boundary layer leads to a decrease of the thermal resistance and an increase of heat losses. In comparison with the helium gas, no saturation is observed because the sensitivity is very low due to the high gas diffusivity.

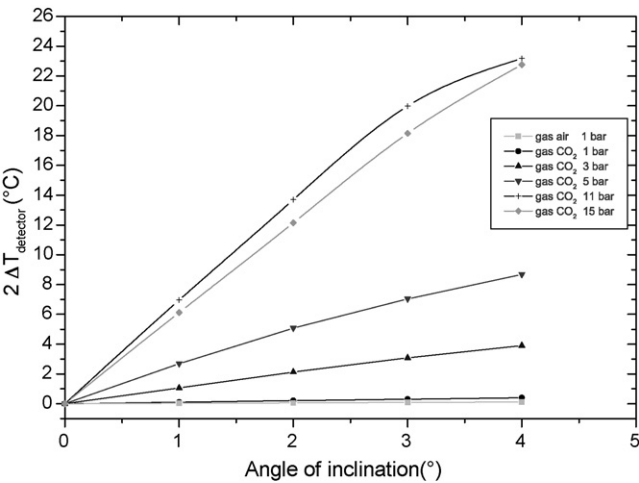


Fig. 6. Sensitivity $2\Delta T_{\text{detector}}$ ($^\circ\text{C}$) vs. tilt sensor (degree).

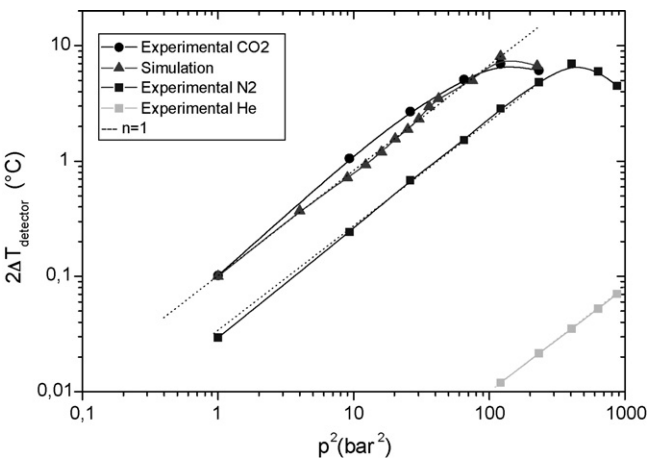


Fig. 7. Sensitivity $2\Delta T_{\text{detector}}$ ($^\circ\text{C}$) vs. square of different gases pressure for 1° of tilt.

In order to understand these phenomena, we introduce two models allowing theoretically evaluate the δ_{th} size. Firstly, we associate the heater size ($100 \mu\text{m}$) to a horizontal hotplate heated up to L size. The relation between the convection coefficient and L is given by [10]:

$$h = 1.32 \left[\frac{(T_r - T_{chip})}{L} \right]^{0.25} \quad (8)$$

With $\Delta T = T_r - T_{chip} = 250 \text{ K}$ (T_{chip} is the temperature on the silicon substrate), $L = 100 \mu\text{m}$, h equal to $52.48 \text{ (W/m}^2 \text{ K)}$.

The thermal boundary layer size is given by: $\delta_{th} = (\lambda/h)$. For example, at 563 K for CO_2 gas at atmospheric pressure, $\lambda = 38.608 \times 10^{-3} \text{ W/m K}$. Finally, we obtain an approximation of the thermal boundary layer size equal to $735 \mu\text{m}$.

Secondly we try to estimate δ_{th} by using the adimensional number approach. An empirical formula for laminar flows on vertical plates is given by [10]:

$$Nu_L = 0.54(Gr_L \times Pr)^{0.25} \quad (9)$$

with

$$Gr_L = \frac{\rho^2 g \beta (T_p - T_0) L^3}{\mu^2} \quad (10)$$

For gas at atmospheric pressure:

$$Pr = \frac{\mu C_p}{\lambda} \quad (11)$$

with μ , cinematic viscosity, C_p , specific heat, λ , thermal conductivity,

For example, with the CO_2 gas with $(T_p - T_0) = 250 \text{ K}$, $Pr = 0.725$, $Gr_L = 5.45 \times 10^{-3}$, $Nu_L = 0.135$.

By using the Nusselt number:

$$Nu = \frac{hL}{\lambda} \quad (12)$$

We determine the coefficient of natural convection equivalent to $51 \text{ W/m}^2 \text{ K}$ for the condition quote here above. The δ_{th} size is equal to $757 \mu\text{m}$. So, we can obtain a good approximation of the thermal boundary layer size equal to $746 \pm 10 \mu\text{m}$ with these two models, but not evaluate the influence of the pressure on it. Furthermore, we were taking into account that the thermal boundary layer is proportional to the square root of gas diffusivity and inversely proportional to the square root of gas pressure [9]. By using these properties, we theoretical evaluate the evolution of the thermal boundary layer size with different gas pressure.

$$\delta_{th} = \frac{\sqrt{a}}{(g\beta\Delta T)^{1/4}} \quad (13)$$

δ_{th} is also limited by the cavity size. Accounting for different gas diffusivity from 1 to 30 bar we represent the variation of δ_{th} function of the gas pressure on Fig. 8. From 1 to 9 bar, the detectors are inside the thermal boundary layer for the CO_2 gas and the sensitivity is linearly proportional to the square of the gas pressure. For pressure larger than 11 bar the detectors are outside the thermal boundary layer so the sensitivity will decrease.

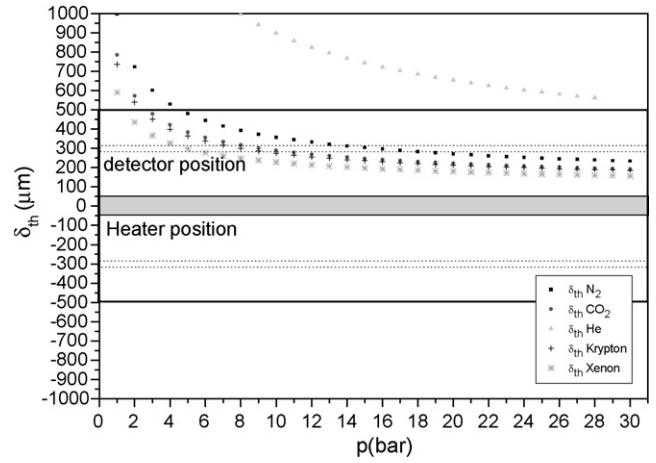


Fig. 8. Theoretical thermal boundary layer variations vs. different gases pressure.

So, the thermal boundary layer size is limited by the etched of the cavity and decreases when the gas pressure increases. However, if we use a high gas density like's xenon, the sensitivity will increase up to 5 bar and reaches the maximum between 5 and 6 bar. Then, it will decreases for the same reason. For other gas with higher densities, we assume that a real decrease of the sensor signal will be observed at 2 bar.

The optimum sensitivity for this inclinometer geometry seems to be between 9 and 11 bar for CO_2 gas and between 19 and 21 bar for nitrogen. The experimental and simulation results confirm the analytical solution and the maximum of sensitivity obtained at 11 bar pressure for CO_2 gas pressure.

4.2. Numerical optimization of the sensitivity with the detectors position and the CO_2 gas pressure

For this study, we choose the CO_2 gas for example, which is a good compromise between the sensitivity and readiness in order to compare with the experimental results. As we have seen previously, the pressure in the cavity enclosure is an important factor to determine the gradient shape because it specifies the local gas density in the sensor and the heat quantities per unit of volume. If the pressure grows, the heat density and the thermal boundary layer will be confined in a smaller volume. So the optimum detector's position is modified.

A numerically solution has been investigated in order to measure the detector's position which will give the best sensitivity value between the two detectors for CO_2 gas.

Fig. 9 presents the normalized temperature profile $\Delta T(x)$ for a constant heater temperature rise of $\Delta T = 250 \text{ K}$ for different pressures from 1 to 15 bar. We assume that the temperature rise is close to zero for $x = 1000 \text{ mm}$ or that the thermal boundary layer is limited by the cavity wall. Fig. 10 gives the displacement of the maximum of the detector's sensitivity from 370 to $285 \mu\text{m}$ when the pressure increases from 1 to 15 bar.

So, we can conclude that this inclinometer structure is optimized at 11 bar because the optimum position is $303 \mu\text{m}$ and the

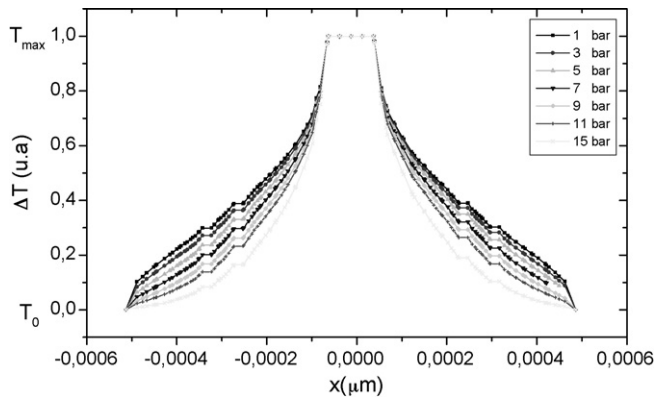


Fig. 9. Temperature profile $\Delta T(x)$ for a constant heater temperature rise $\Delta T = 250$ K and different CO_2 gas under pressure from 1 to 15 bar.

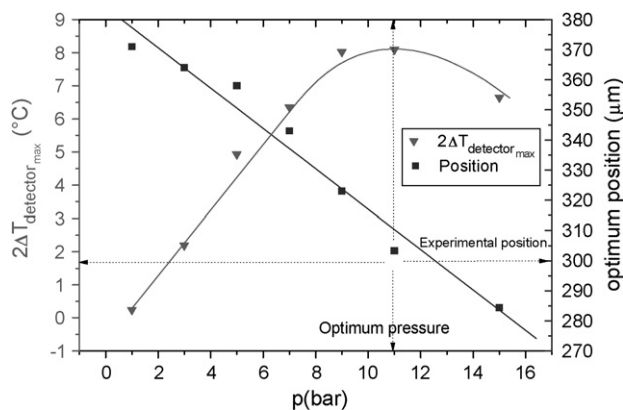


Fig. 10. Optimization of the optimum detector's position and the thermal temperature difference ($2\Delta T_{\text{detector}}$) for different pressure from 1 to 15 bar.

detector's sensitivity equal to 8.1°C per degree of inclination. These results are in a good accordance with experience where the real distance and the sensitivity are respectively $300\ \mu\text{m}$ and 7°C per degree.

5. Conclusion

Temperature profile in an inclinometer based on thermal exchange has been simulated and experimentally investigated as a function of CO_2 gas pressure. The sensor was micromachined by using micro-electronic techniques. To corroborate experimental results, the simulation's results have confirmed that the maximum of sensitivity by using CO_2 gas is at 11 bar.

The theoretical model of the thermal boundary layer has been extended to other gas and experimentally verify and shown that the sensitivity decreases when the detector is outside the thermal boundary layer. The simulation results has shown for different pressure that the optimum detector's position depends on the evolution of the gradient shape and a displacement of the optimum sensitivity from 370 to $285\ \mu\text{m}$ is observed when the pressure increases from 1 to 15 bar for CO_2 gas. Very high sensitivity has been experimentally and numerically obtained, respectively of 7°C and 8.1°C per angle of inclination.

Finally, sub-micron g sensitivity could be achieved also by optimizing the structure, so the detector's position inside the cavity for higher pressure, the cavity volume or the gas nature with higher sensitivity likes oil.

Acknowledgements

The authors would like to acknowledge the work of Mr. M. Degea, F. Cano and Mrs. V. Coronato for their technical assistance.

References

- [1] Lapadatu, D. Habibi, S. Reppen, B. Salomonsen, G. Kvisteroy, Dual-axes capacitive inclinometer/low g accelerometer for automotive applications, IEEE Int. Micro Electro-Mechanical Systems, Interlaken, Switzerland, January 21–25, 2001.
- [2] U. Mescheder, S. Majer, Micromechanical inclinometer, Sens. Actuators A 60 (1997) 134–138.
- [3] R. Dao, D.E. Morgan, H.H. Kries, D.M. Bachelder, Convective accelerometer and inclinometer, US Patent 5,581,034 (1996).
- [4] A.M. Leung, J. Jones, E. Czyzewska, J. Chen, M. Pascal, Micromachined accelerometer with no proof mass, Technical Digest of Int. Electron Device Meeting (IEDM97), 1997, pp. 899–902.
- [5] V. Milanovic, E. Bowen, M.E. Zaghoul, N.H. Tea, J.S. Suehle, B. Payne, M. Gaitan, Micromachined convective accelerometers in standard integrated circuits technology, Appl. Phys. Lett. 76 (2000) 4.
- [6] S. Billat, H. Glosch, M. Kunze, F. Hedrich, J. Frech, W. Lang, Micromachined inclinometer with high sensitivity and very good stability, Sens. Actuators A 3211 (2002) 1–6.
- [7] F. Mailly, A. Giani, A. Martinez, R. Bonnot, P. Temple-Boyer, A. Boyer, Micromachined thermal accelerometer, Sens. Actuators A 103 (2003) 359–363.
- [8] P. Temple-Boyer, C. Rossi, E. Saint-Etienne, E. Scheid, Residual stress in low pressure chemical vapor deposition SiN_x films deposited from silane and ammonia, J. Vac. Sci. Technol. A 16 (4) (1998) 2003–2007.
- [9] F. Mailly, A. Martinez, A. Giani, F. Pascal-Delannoy, A. Boyer, Effect of gas pressure on the sensitivity of a micromachined thermal accelerometer, Sens. Actuators A 109 (2003) 88–94.
- [10] B. Eyglument, Manuel de la thermique: théorie et pratique, second ed., Hermès, France, 1997, pp. 154–155.

Biographies

Johann Courteaud was born in Reunion Island. He received his PhD in electronics optronics and systems from the University of Montpellier, France, in 2006. Since then, he works on modellization, electronics characterizations and optimization of thermal micro sensors structures.

Phillippe Combette received his PhD in electronics optronics and systems from the University of Montpellier, France, in 2000. Since then, he works in the center of electronic and micro-optoelectronic of Montpellier University, where he is a specialist on piezoelectricity. Presently, he is involved in pyroelectricity sensors for thermal flow measurements and others applications.

Nicolas Crespy was born in Carcassonne, France. He received the "Doctorat" degree in Electronics from Montpellier University in 2005. Since then, he has been preparing a PhD thesis on "Studies and characterization of a thermal accelerometer" in the center of Electronic and Micro-Optoelectronic of Montpellier University where he works on studies of electronics characterizations and optimization of silicon micro accelerometers structures.

Guy Cathebras received the French engineer degree in 1984 from the École Nationale Supérieure de l'Électronique et de ses Applications, the "Diplôme de Doctorat" in 1990 and the "Habilitation à Diriger les Recherches" in 2005 from the Montpellier II University. Since 1992, he is an assistant professor at the Ecole

Polytechnique Universitaire de Montpellier and a researcher of the Laboratoire d'Informatique, Robotique et Microelectronique de Montpellier (LIRMM). His research interests include biomedical devices with special emphasis on Functional Electrical Stimulation systems and ENG detection. More generally, he is interested by CMOS analog design, especially for tricky or unconventional devices.

Alain Giani was born in Arles, France. He received his PhD in electronics optronics and systems from the University of Montpellier, France, in 1992. Since then, he works in the center of Electronic and Micro-Optoelectronic of Montpellier University, where he is a specialist on vacuum deposition engineering. Presently, he is involved in thermal sensors for flow measurements and optoelectronics applications.